

## Correlation of Cs flux and work function of a converter surface during long plasma exposure for negative ion sources in view of ITER

Sofia Cristofaro, Roland Friedl, Ursel Fantz

### Angaben zur Veröffentlichung / Publication details:

Cristofaro, Sofia, Roland Friedl, and Ursel Fantz. 2020. "Correlation of Cs flux and work function of a converter surface during long plasma exposure for negative ion sources in view of ITER." *Plasma Research Express* 2 (3): 035009.  
<https://doi.org/10.1088/2516-1067/abae81>.

PAPER • OPEN ACCESS

# Correlation of Cs flux and work function of a converter surface during long plasma exposure for negative ion sources in view of ITER

## Recent citations

- [Effect of a low pressure low temperature hydrogen plasma on the work function of europium](#)  
Sofia Cristofaro *et al*

To cite this article: S Cristofaro *et al* 2020 *Plasma Res. Express* **2** 035009

View the [article online](#) for updates and enhancements.

## Plasma Research Express



## PAPER

## OPEN ACCESS

RECEIVED  
9 July 2020REVISED  
22 July 2020ACCEPTED FOR PUBLICATION  
12 August 2020PUBLISHED  
21 August 2020

Original content from this work may be used under the terms of the [Creative Commons Attribution 4.0 licence](#).

Any further distribution of this work must maintain attribution to the author(s) and the title of the work, journal citation and DOI.



## Correlation of Cs flux and work function of a converter surface during long plasma exposure for negative ion sources in view of ITER

S Cristofaro<sup>1,2</sup> , R Friedl<sup>2</sup> and U Fantz<sup>1,2</sup> <sup>1</sup> Max-Planck-Institut für Plasmaphysik, Boltzmannstr. 2, D-85748 Garching, Germany<sup>2</sup> AG Experimentelle Plasmaphysik, Universität Augsburg, D-86135 Augsburg, GermanyE-mail: [sofia.cristofaro@ipp.mpg.de](mailto:sofia.cristofaro@ipp.mpg.de)**Keywords:** negative hydrogen ions, caesium, NNBI

## Abstract

Negative hydrogen ion sources for NBI systems at fusion devices rely on the surface conversion of hydrogen atoms and positive ions to negative hydrogen ions. In these sources the surface work function is decreased by adsorption of caesium (work function of 2.1 eV), enhancing consequently the negative ion yield. However, the performance of the ion source decreases during plasma pulses up to one hour, suggesting a deterioration of the work function. Fundamental investigations are performed in a laboratory experiment in order to study the impact of the plasma on the work function of a freshly caesiated stainless steel surface. A work function of 2.1 eV is achieved in the first 10 s of plasma, while further plasma exposure leads to the removal of Cs from the surface and to the change of the work function: a value of around 1.8–1.9 eV is measured after 10–15 min of plasma exposure and then the work function increases, approaching the work function of the substrate ( $\geq 4.2$  eV) after 5 h. The Cs removal must be counteracted by continuous Cs evaporation, and investigations performed varying the Cs flux towards the surface have shown that a Cs flux of at least  $1.5 \times 10^{16} \text{ m}^{-2} \text{ s}^{-1}$  is required to maintain a work function of 2.1 eV during long plasma exposure at the laboratory experiment.

## 1. Introduction

The neutral beam injection systems for ITER will be based on negative hydrogen ions (NNBI) [1–3], and the corresponding negative hydrogen and deuterium ion source must deliver a homogeneous and high energy beam with pulses of up to one hour at a gas pressure of 0.3 Pa. The ion source must deliver an extracted negative ion current density of  $329 \text{ A m}^{-2}$  for hydrogen ( $286 \text{ A m}^{-2}$  for deuterium) over an ion source area of  $1 \times 2 \text{ m}^2$ , with a co-extracted electron current below the extracted negative ion current. In order to fulfill these strict requirements, the negative ion source relies on the surface conversion of hydrogen atoms and positive ions into negative hydrogen ions by electron transfer from a low work function surface [4]. In the plasma sheath, whose thickness is on the order of few Debye lengths and is far below the millimeter, the surface created negative ions repel the electrons, which become the minority species [5, 6]. Consequently, the co-extracted electron current decreases. The plasma grid, which is the first grid of the extraction and acceleration system and acts as converter surface, is made of molybdenum coated copper, and caesium is continuously evaporated inside the source to reduce the surface work function. Caesium is, in fact, the alkali metal with the lowest work function among all stable elements, i.e. 2.1 eV [7]. The work function of a caesiated metallic surface depends on the Cs coverage: in ultra-high vacuum systems ( $\leq 10^{-9}$  mbar) the work function of a clean metallic surface (typically around 4–5 eV [7]) decreases with increasing Cs coverage, until it reaches a minimum around 1.4–1.8 eV at 0.5–0.8 monolayer (ML) depending on the substrate material and on the crystallographic orientation [8–10]. The work function then increases again, until the bulk Cs work function of 2.1 eV is obtained and maintained for coverages above few monolayers.

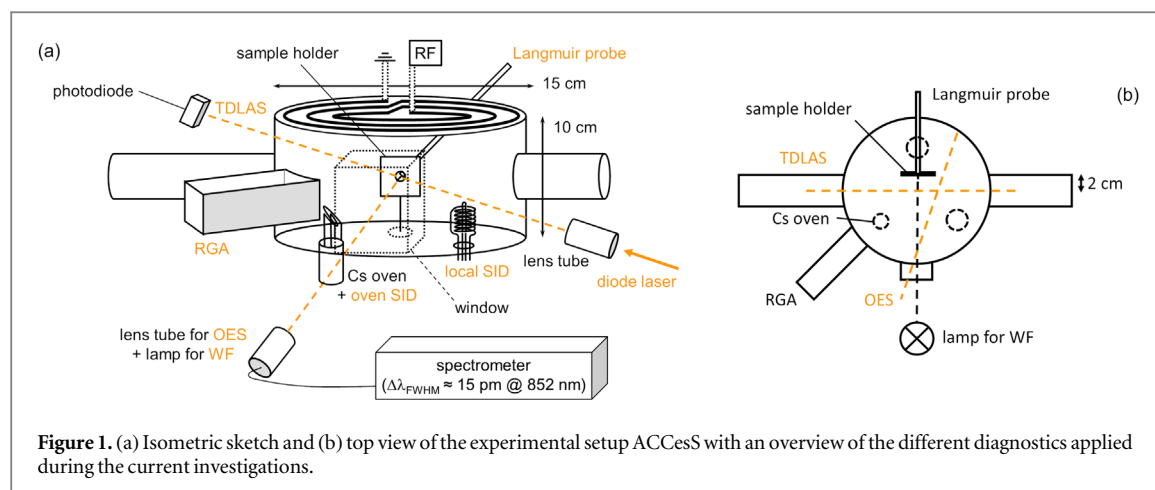
The test facility ELISE is equipped with an RF-driven source half of the size of the ITER source, and it has the aim to demonstrate the feasibility to fulfill the ITER requirements during long pulse operation [5, 11]. The background pressure is of  $10^{-7}$ – $10^{-6}$  mbar [11]. The operation is mainly limited by the unstable co-extracted electron current, which strongly increases during long pulses up to values harmful for the extraction system [12]. This is particularly evident during deuterium operation, where the co-extracted electron current is higher and shows a stronger temporal dynamics with respect to hydrogen operation [12]. A possible explanation of the increase of the co-extracted electron current during long pulse operation is a change of the surface conditions of the plasma grid: if the flux of surface created negative ions into the plasma slightly decreases due to changes of the Cs layer and of the work function, the electron flux towards the grid system would consequently increase. The relative change, even if negligible for the negative ions, would be much more relevant for the electrons since they are the minority species. Due to the dependence of the work function on the Cs coverage, maintaining a Cs layer above few monolayers would allow to maintain a constant work function of 2.1 eV. However, during long pulses a decrease of the neutral Cs density is observed in front of the plasma grid [13], suggesting that the Cs flux towards the surface (typically  $10^{16}$ – $10^{17}$  m<sup>-2</sup>s<sup>-1</sup>) is not enough to maintain a Cs layer above few monolayers. When the hydrogen plasma is applied in front of the caesiated surface (typical electron density  $n_e \sim 10^{16}$ – $10^{17}$  m<sup>-3</sup> and temperature  $T_e \sim 1$ –2 eV in front of the plasma grid), interactions of the plasma species with the surface—like adsorption, erosion, physical sputtering, and chemical surface reactions—can take place. The plasma particles such as atomic hydrogen and positive hydrogen ions impinging on the surface can lead to physical sputtering and/or chemical reactions (atomic hydrogen for instance is a radical which can initiate a multitude of chemical reactions), and the UV/VUV radiation may contribute to surface modifications. All these mechanisms can thus lead to changes of the work function. Typical fluxes of atomic hydrogen ( $\Gamma_H$ ) and positive ions ( $\Gamma_+$ ) can be estimated from measurements shown in [14–17] and are in the range of  $2$ – $5 \times 10^2$  m<sup>-2</sup>s<sup>-1</sup> and  $5$ – $12 \times 10^{20}$  m<sup>-2</sup>s<sup>-1</sup>, respectively. The potential drop at the surface is typically of few volts, and it determines the maximum energy of the impinging positive ions. The flux of VUV photons towards the surface (with energies between 3 and 15 eV) is expected to be on the same order of magnitude as the positive ion flux, as observed in [18]. Additionally, the plasma heats the surface, hence thermal effects take place simultaneously. Consequently, removal and redistribution of Cs (or Cs compounds) from the surfaces occur [19] and influence the work function. Maintaining a constant and homogeneous low work function at the caesiated plasma grid is thus the key parameter to ensure good performance of the negative ion source.

Measurements of the plasma grid work function at the ion sources are highly desirable to confirm the deterioration of the work function during long plasma exposure, but unfortunately they lack often of accessibility. Some investigations on the work function of caesiated surfaces at arc ion sources are shown in [20–23], where hot tungsten filaments are applied to ignite the plasma with consequent deposition of tungsten in the Cs layer. In these contributions, the work function was measured after short pulses (below one minute).

In the present work, absolute measurements of work function of a caesiated surface are performed in an ICP experiment in order to study the impact of hydrogen plasma exposure on the surface work function. A previous study [24] was focused on the impact of the plasma exposure on the work function of a degraded Cs layer on a stainless steel surface (initial work function of 3.0 eV): the hydrogen plasma decreased the work function down to 2.5 eV after 3 h of plasma exposure, and a work function of  $2.2 \pm 0.1$  eV was achieved only with additional Cs evaporation during hydrogen plasma and high Cs fluxes on the order of  $10^{17}$  m<sup>-2</sup>s<sup>-1</sup>. However, in the ion source the plasma grid is caesiated with fresh Cs before the plasma pulse. Hence, in this contribution, the case of a freshly caesiated stainless steel sample is studied for a comparison with the degraded Cs layer studied in [24]. Consequently, the plasma exposure is here initiated shortly after caesiation of the sample (initial work function of 2.7 eV, reproducible with the measurements shown in [24] after caesiation in vacuum). Finally, a section about the transfer of the results to ion sources is presented.

## 2. Experimental setup

The flexible laboratory experiment ACCesS (Augsburg Comprehensive Cesium Setup) [24, 25] consists of a cylindrical stainless steel vessel with a diameter of 15 cm and a height of 10 cm, as shown in figure 1. The background pressure within the vessel is on the order of  $10^{-6}$  mbar. The plasma is generated via inductive RF coupling (frequency 27.12 MHz, maximal RF power 600 W) using a planar coil located on the top of the vessel. The accessible pressure range for operation in hydrogen or deuterium is from 2 to 20 Pa. The vessel walls are temperature controlled by water to limit the temperature during plasma operation below 40 °C. Caesium is introduced into the experiment by a Cs oven located at the bottom plate and containing a liquid Cs reservoir, assuring stable and controlled evaporation of pure Cs. The sample holder is positioned near the center of the experimental chamber, and it is electrically and thermally insulated from the vessel. Samples are clamped to the sample holder with screwable stainless steel clamps such that the sample surface is facing the center of the



experiment. The temperature of the sample surface is monitored by means of a thermocouple clamped on the front side of the sample. For the investigations presented here, the chamber is filled with hydrogen or deuterium gas at a pressure of 10 Pa (gas flow of 10 sccm), and the RF power is set to 250 W.

## 2.1. Diagnostics

Several diagnostic systems for Cs detection surround the sample: two surface ionization detectors (SID) monitor the Cs outflow from the oven and the redistribution in the vessel in vacuum [26], while the neutral Cs density is absolutely measured by tunable diode laser absorption spectroscopy (TDLAS) averaged along the diagonal line of sight in vacuum and plasma environment [27, 28]. The TDLAS line of sight is parallel to the sample holder at 2 cm distance. The detection limit for the Cs density measurement is  $n_{Cs} \geq 2 \times 10^{13} \text{ m}^{-3}$ , and the measured Cs density has an error of typically  $\pm 10\%$  (for densities close to the detection limit the error increases up to  $\pm 50\%$  due to the low signal-to-noise ratio).

During plasma operation optical emission spectroscopy (OES) is applied for monitoring the Cs emission and the plasma parameters [29], e.g. the gas temperature, the atomic hydrogen density, the electron density, and the electron temperature, averaged along the line of sight crossing the vessel as shown in the top view in figure 1. Local measurements of electron density and electron temperature, as well as the electrostatic potentials, are obtained by a movable Langmuir probe in vicinity of the surface. Finally, a non-calibrated residual gas analyzer (RGA) is used to monitor the background gases during operation. Details on the applied diagnostics (OES, Langmuir probe, and RGA) can be found in [30]. Due to the high Cs dynamics during plasma operations, all diagnostics are operated simultaneously in order to relate the different parameters to the same experimental condition.

## 2.2. Work function diagnostic

The work function (WF) of the sample is evaluated considering the photoelectric effect induced by irradiation and by applying the Fowler method [31] by means of the enhanced procedure described in [32]. A high pressure mercury lamp (100 W) is applied as a broadband light source since it has a highly intense emission from UV throughout the visible range. The light passes through an interference filter and is focused on the sample holder resulting in a spot diameter of about 1.5 cm. The photoemitted electrons are collected at the vessel walls by applying a bias voltage of  $-30 \text{ V}$  to the sample against the grounded walls. The photocurrents are measured by a Keithley 602 Electrometer, capable of measuring currents down to the pA range. The dark current is between  $10^{-10} \text{ A}$  in vacuum and  $10^{-6} \text{ A}$  after plasma with Cs evaporation. The photocurrent depends on the energy of the incident photons, on the temperature of the sample, and on the work function  $\chi$  of the surface. Hence, by using different interference filters to select the photon energy and by measuring the corresponding photocurrents, it is possible to absolutely determine the work function. Twenty filters with central transmission wavelength between 239 and 852 nm and with a nominal FWHM of 10 nm are available for the current investigations. This set of filters consists of 11 more filters with respect to the set applied in [24], fulfilling the conditions explained in [32]. Consequently, photon energies down to 1.45 eV are now available, but the lowest work function value to be detected depends on the signal-to-noise ratio. The entire setup was calibrated by means of an absolutely calibrated spectrometer and a radiant power meter.

Measurement of the photocurrent is not possible during plasma operation, since the plasma electrons will contribute to the measured current and it will not be possible to discern the low photocurrents from the total current. Consequently, the work function is measured within the first minutes (max. 3 min) after switching off

the plasma. Hence, plasma pulses are used with plasma-on time ranging from few seconds up to several hours, and they are interrupted by short gas phases in order to measure the work function. The gas phases must be as short as possible in order to avoid degradation effects on the work function of the sample [24]. Typically, 5–10 min are enough to measure the work function few times after each plasma pulse. The typical error of the evaluated work function is of 0.1 eV. However, it must be considered that the values evaluated via the Fowler method are always upper limits, as explained in [32].

### 3. Results and discussion

Stainless steel was chosen as testing material due to its machinability, and investigations have shown that at least in vacuum the substrate has only negligible impact on the work function [24]. Hence, in order to be reproducible with former investigations and to have the possibility to directly compare with the former results for a degraded Cs layer in plasma [24, 32], stainless steel is used also during this campaign. Since the campaigns here were performed in parallel with measurements using cavity ring-down spectroscopy for the detection of  $\text{H}^-$  [25], samples of different lengths  $l$  from 30 to 140 mm (with a height of 30 mm and thickness of 1 mm) were used. The different size of the samples does not lead to significant variations of the plasma parameters measured by the Langmuir probe above the surface in the center of the sample.

For each sample, the same preparation procedure has been followed in order to assure reproducibility. In order to clean the sample from air adsorbates deposited during the sample installation, the sample surface is first exposed to a hydrogen plasma for 5 h, reaching a surface temperature of 225 °C and achieving a work function of around 4.5 eV (clean stainless steel). The caesiation of the sample takes place in vacuum, and is stopped once a work function of 2.7 eV is reached. The Cs density at this point is measured to be about  $2 \times 10^{14} \text{ m}^{-3}$ . For the determination of the Cs flux onto the surface, which is the relevant parameter for ion sources, uniform redistribution within the vessel is assumed. Consequently, the undirected flux of the Cs atoms is taken as  $1/4 n_{\text{Cs}} v$ , where the temperature of Cs (around 500–550 K) is used for the thermal velocity  $v$ , resulting in a flux on the order of  $10^{16} \text{ m}^{-2}\text{s}^{-1}$ . Cs is easily getterd by impurities (for instance water and oxygen) as well as by hydrogen due to its high chemical reactivity, and several Cs compounds may be formed at the surface, as for example CsH, CsOH and Cs oxides, which are stable with negative formation enthalpies from 0.56 eV for CsH (which decomposes at around 180 °C at 10 Pa [33]) up to several eV for the other compounds [34]. Unfortunately, neither in vacuum nor in plasma the actual stoichiometric composition is known, nor it can be measured since *in situ* diagnostics are not available at ACCesS.

The starting point in each of the following graphs is a freshly caesiated surface with a work function of 2.7 eV being exposed to a hydrogen discharge at 10 Pa and 250 W with plasma-on times from few seconds up to several hours. Typical plasma parameters are  $T_e \sim 2 \text{ eV}$ ,  $n_e \sim 1.4 \times 10^{16} \text{ m}^{-3}$ ,  $\Gamma_H \sim 1.3 \times 10^{22} \text{ m}^{-2}\text{s}^{-1}$ ,  $\Gamma_+ \sim 1.3 \times 10^{20} \text{ m}^{-2}\text{s}^{-1}$ . The potential drop at the surface is about 8 V, determining the maximum energy of the impinging positive ions, while the temperature of the atoms is assumed equal to the gas temperature (around 0.05 eV) due to the high collision frequencies at the pressure of 10 Pa.

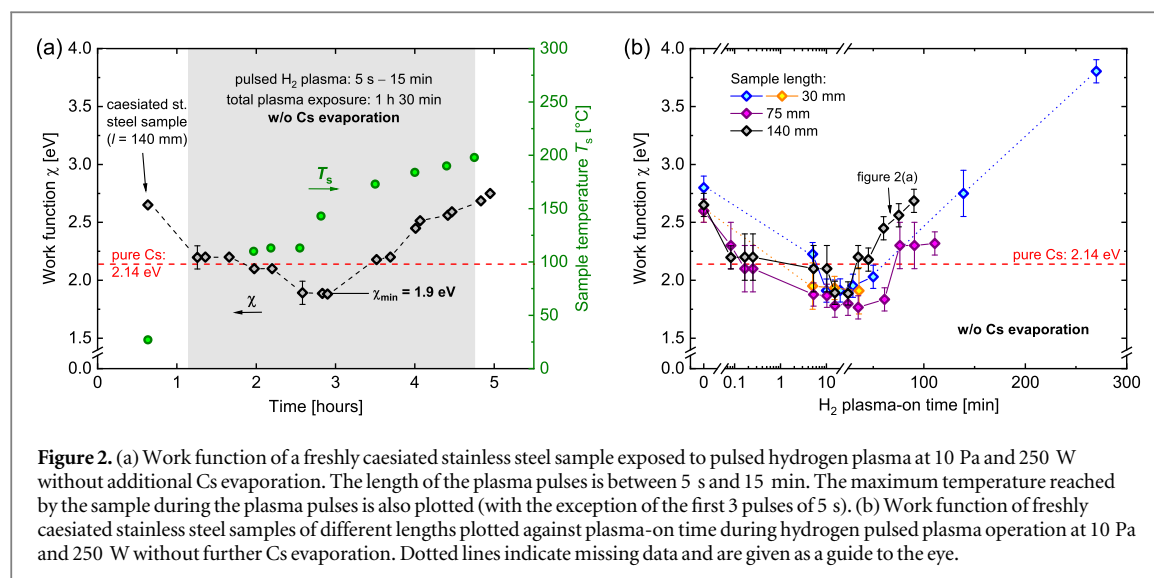
#### 3.1. Work function of a freshly caesiated surface during plasma without further Cs evaporation

Figure 2(a) shows the work function of a freshly caesiated surface (initial work function of 2.7 eV) for a sample of 140 mm length during plasma exposure (indicated by the gray shaded area) without additional Cs evaporation. The maximum temperature of the sample during each plasma pulse is also shown in the figure. At the beginning 3 pulses of 5 s each are applied, and the work function drops from 2.7 to  $2.2 \pm 0.1 \text{ eV}$  already after the first pulse, reaching a value very close to the work function of pure bulk Cs. During the pulse, it was not possible to have a precise measurement of the temperature, but it was below 100 °C. During the first plasma pulses peaks in the RGA signals for  $\text{H}_2\text{O}$ ,  $\text{CO}_2$  and  $\text{N}_2$  are observed, suggesting that the plasma is releasing the adsorbates from the experiment surfaces including the Cs layer. The RGA signals instantaneously decrease when the plasma is switched off, and the magnitude of the peaks decreases during the subsequent plasma pulses, until no RGA peaks are observed after an overall plasma exposure of 15 min.

For the campaign in figure 2(a) the TDLAS was not available, however a reproducible campaign after the installation of the TDLAS diagnostics has shown that the Cs deposited on the surfaces is redistributed inside the experiment when the plasma is on: the Cs density is around  $2 \times 10^{14} \text{ m}^{-3}$  during the first plasma pulse and then decreases from pulse to pulse until the signal reaches the detection limit for the Cs detection ( $\leq 2 \times 10^{13} \text{ m}^{-3}$ ) after a pulsed plasma exposure of more than 1 hour. For each pulse, when the plasma is switched off the Cs density drops.

After the 3 pulses of 5 s, the pulse length is increased step-wise from 5 s to 15 min, interrupting the plasma only to measure the work function. Due to the additional plasma exposure and the interaction of the plasma particles with the surface, the work function first decreases and a minimum work function of  $\chi_{\text{min}} = 1$ .





**Figure 2.** (a) Work function of a freshly caesiated stainless steel sample exposed to pulsed hydrogen plasma at 10 Pa and 250 W without additional Cs evaporation. The length of the plasma pulses is between 5 s and 15 min. The maximum temperature reached by the sample during the plasma pulses is also plotted (with the exception of the first 3 pulses of 5 s). (b) Work function of freshly caesiated stainless steel samples of different lengths plotted against plasma-on time during hydrogen pulsed plasma operation at 10 Pa and 250 W without further Cs evaporation. Dotted lines indicate missing data and are given as a guide to the eye.

**Table 1.** Work function values achieved for a degraded Cs layer [24] and a fresh Cs layer exposed to hydrogen plasma, when no additional Cs is evaporated in the experiment ('without Cs') and when a continuous Cs flux is maintained ('with Cs', see section 3.3).

Experiment	Work function $\chi$ [eV]			References
	Initial value	Without Cs	with Cs	
Degraded Cs layer	3.0	2.5 <sup>a</sup>	2.2	[24]
Fresh Cs layer	2.7	2.1 <sup>b</sup>	2.1	Present paper

<sup>a</sup> After about 3 h of plasma.

<sup>b</sup> For the first few minutes of plasma.

$9 \pm 0.1$  eV is measured after an overall plasma-on time of 15 min. This value is measured with a dark current of  $10^{-9}$  A and might be an upper limit. Then the work function starts to increase reaching 2.7 eV at the end of the present campaign after an overall plasma-on time of 1.5 h.

In further campaigns longer plasma exposures are applied with pulse lengths from several minutes up to few hours. The longer plasma exposure leads to a further increase of the work function, reaching 3.8 eV after an overall plasma-on time of 4.5 h and approaching the work function of a clean stainless steel surface ( $\geq 4.2$  eV) after more than 5 h of plasma.

Figure 2(b) shows the work function plotted against the plasma-on time for a group of similar campaigns performed with different samples of stainless steel. All the samples show a first decrease of the work function from 2.7 eV down to 2.1 eV within 10 s of plasma-on time and a minimum value measured between 1.8 and 1.9 eV at around 10–15 min of plasma exposure. All the samples then show an increase of the work function up to values much higher than 2.1 eV.

In contrast to a degraded Cs layer [24], a freshly caesiated surface shows a work function equal to the one of pure Cs (2.1 eV) after only 5–10 s of plasma exposure without the need for further Cs evaporation. A decrease of the work function was observed in [24] for a degraded Cs layer (initial work function of 3.0 eV), however it was not possible to achieve the work function of bulk Cs by exposing the surface to the plasma even for about 3 h. Fresh Cs evaporation was needed to achieve low work functions of 2.2 eV (see table 1 which summarizes the work functions achieved at ACCesS during plasma exposure).

The temporal variation of the work function due to plasma exposure is the most important result of this study. The observation of a minimum work function is either due to a Cs coverage below one monolayer on the sample surface or to the adsorption of hydrogen particles on the Cs layer. Regarding the former effect, the minimum value that is usually reached in ultra-high vacuum systems for some sub-monolayer of Cs coverage is between 1.4 and 1.8 eV [8–10]. These values are lower with respect to the one evaluated here, however none of the literature values refers to a stainless steel substrate and a moderate vacuum level. Additionally, the value

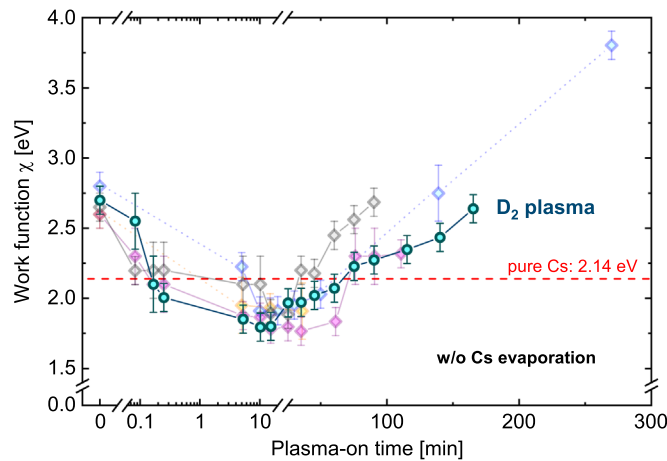


**Figure 3.** Work function of a freshly caesiated stainless steel sample ( $l = 140$  mm) plotted against plasma-on time during pulsed deuterium plasma operation at 10 Pa and 250 W without further Cs evaporation. The data referring to hydrogen from figure 2(b) is plotted transparently in the background.

measured here can be an upper limit due to the evaluation via the Fowler method. Regarding the adsorption of hydrogen, it was observed in [35] that the hydrogen adsorption on a clean Cs monolayer decreases the work function by few 0.1 eV, which is comparable with the measurements obtained at ACCesS. Hence, both the adsorption of H atoms in the Cs layer and the presence of a sub-monolayer of Cs on the surface would explain a lower work function with respect to the bulk Cs value.

Nonetheless, the investigations performed here clearly show that for plasma exposures of few hours the work function increases up to values close to the clean substrate work function. The behavior of the work function can be explained by a gradual removal of the Cs layer from the surface due to the chemical, thermal and photo-induced desorption (the impinging positive ions and UV/VUV photons have higher energies than the binding energy of Cs at the surface, which is between 0.8 eV [34] and 3.3 eV [36] depending on the Cs coverage). Moreover, for plasma-on time larger than 20 min the sample temperature is higher than 175 °C so CsH can be decomposed, which might lead to desorption of Cs [33]. Hence, Cs removal is possible and is the most probable explanation for the observed behavior.

While the samples reach  $\chi_{\min}$  at approximately the same time, during the phase of increasing work function the samples show different values of work function under the same plasma-on time. This might be due to a difference in the initial thickness of the Cs layer (impossible to determine): while the dominant process for the observed minimum work function can be the hydrogen adsorption rather than the Cs removal, the dominant process for plasma-on times above 20 minute is the Cs removal, hence different thickness of the layer would lead to different onsets of the work function increase.

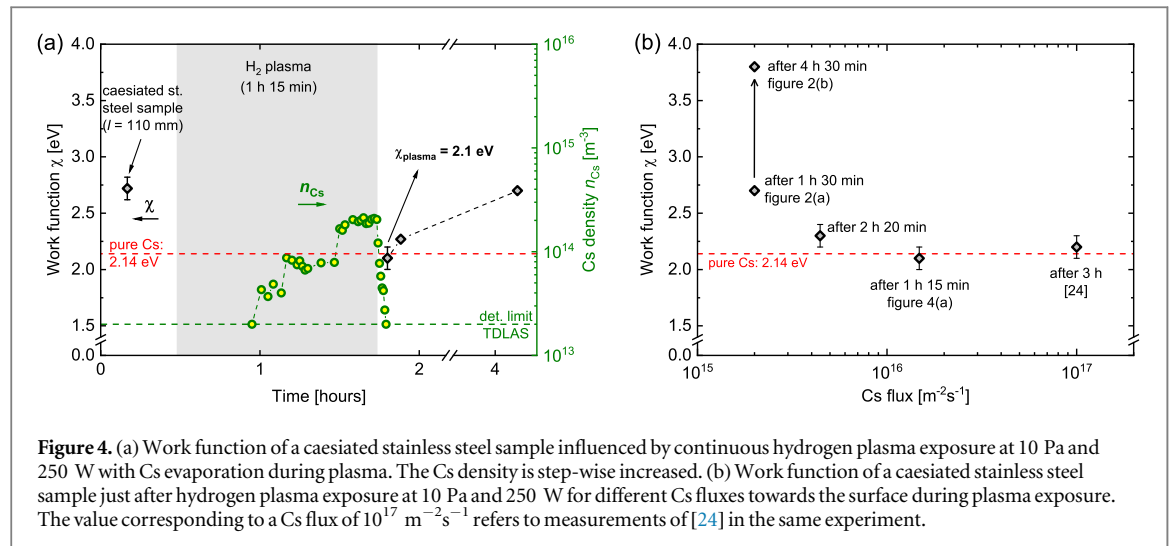
The increase of the work function due to Cs removal is a critical issue, however it is not possible to discriminate which mechanism (or which combination of mechanisms) is responsible for the Cs removal. While thermal and chemical effects are isotopically independent, physical sputtering is related to the mass, hence using a deuterium plasma could help to narrow down possible surface processes responsible for the Cs removal, as shown in the following.

### 3.2. Comparison to deuterium plasma operation

Typical plasma parameters of a deuterium plasma at 10 Pa and 250 W are similar as for hydrogen, e.g.  $n_e \sim 2 \times 10^{16} \text{ m}^{-3}$ ,  $T_e \sim 2 \text{ eV}$ ,  $\Gamma_D \sim 1.3 \times 10^{22} \text{ m}^{-2}\text{s}^{-1}$ , and  $\Gamma_+ \sim 1.2 \times 10^{20} \text{ m}^{-2}\text{s}^{-1}$ . The potential drop at the sample surface is of 11 V, and the gas temperature is around 0.05 eV. The maximal temperature reached by the sample is 275 °C, higher with respect to hydrogen operation, hence it might lead to an enhanced thermal desorption and thermal decomposition of CsD. Furthermore, due to the higher mass of the impinging particles, the physical sputtering is expected to be more relevant than in hydrogen. Consequently, if these are the driving processes for the Cs removal, a faster change of the work function can be expected in deuterium.

Figure 3 shows the work function of a freshly caesiated surface ( $l = 140$  mm) plotted against the plasma exposure time in deuterium without further Cs evaporation together with the results obtained in hydrogen from figure 2(b). The work function of a pure Cs layer (2.1 eV) is reached between 5 and 10 s of plasma exposure while a minimum work function of 1.8 eV is measured after 10 min. Then the work function of the surface increases up to 2.6 eV after almost 3 h of plasma exposure.





Comparing hydrogen and deuterium operation, the bulk Cs work function is achieved for both plasmas within 10 s and a similar minimum value is observed at the same plasma-on time (around 10 min), hence no significant isotopic effect occurs here. However, the increase of the work function due to Cs removal is lower in deuterium (around +0.3 eV/h) than in hydrogen plasma (around +0.5 eV/h). Hence, thermal desorption, thermal decomposition of Cs hydride and the physical sputtering do not seem to be the driving processes of the Cs removal, since these mechanisms are enhanced in deuterium and should have lead to a faster increase of the work function with respect to hydrogen operation. The results suggest that the driving process is thus chemical.

### 3.3. Cs flux dependent work function measurements during continuous plasma exposure

During long plasma operation at the ion source, Cs is expected to be continuously removed from the surfaces leading to a work function degradation of the plasma grid. Hence, it is mandatory to maintain a sufficient Cs flux onto the surface during plasma to counteract the Cs removal. The aim is to achieve and maintain several Cs layers on the surface, resulting in a work function of 2.1 eV. In this case, in fact, the work function is independent of the thickness of the layer, assuring temporal stability and homogeneity over the entire big area of the plasma grid.

At ACCeS, the case of a high Cs flux ( $> 10^{17} \text{ m}^{-2} \text{ s}^{-1}$ ) during plasma was studied in [24]: this flux allows to maintain a work function of 2.2–2.3 eV for almost 3 h. However, for the current investigations the range of low Cs fluxes is studied in order to determine the threshold value for ensuring a stable low work function. In order to study this case, a stainless steel sample is caesiated in vacuum achieving a work function of 2.7 eV. The caesiation is then stopped, and a continuous hydrogen plasma at 10 Pa and 250 W is applied. During the plasma exposure Cs evaporation is resumed, and the Cs density is slowly increased step-wise. In order to measure the work function, the plasma is stopped as well as the Cs evaporation. The whole procedure must be repeated (starting always from a clean stainless steel sample) to measure the work function for different values of Cs flux, requiring several days for a single measurement.

Figure 4(a) shows the work function of a freshly caesiated stainless steel sample ( $l = 110$  mm, work function of 2.7 eV) and the Cs density measured by TDLAS during the procedure described above. The caesiation is stopped before applying the hydrogen plasma, and during the continuous plasma exposure of 1 hour and 15 min further fresh Cs is evaporated into the vessel, without stopping to measure the work function. The Cs density measured by TDLAS is increased step-wise up to the stable value of  $2 \times 10^{14} \text{ m}^{-3}$ , corresponding to a Cs flux towards the surface of  $1.5 \times 10^{16} \text{ m}^{-2} \text{ s}^{-1}$ . When the plasma is switched off, also the Cs evaporation in the vessel is stopped. The work function is measured within few minutes after plasma equal to 2.1 eV. In comparison with the hydrogen campaigns without Cs evaporation of figure 2(b), the work function is expected to reach values higher than 2.3 eV after 75 min of plasma exposure.

In figure 4(a), the typical work function degradation after plasma exposure can be observed: the work function increases from 2.1 to 2.7 eV after 2 h resulting in a degradation rate of +0.3 eV/h, comparable to the value observed in [24] (+0.4 eV/h).

In order to determine the minimum Cs flux required to maintain a temporally stable work function of 2.1 eV, the same caesiation procedure is repeated with different Cs densities during plasma. The work function measured after long pulse plasma operation is shown for different Cs fluxes in figure 4(b). The Cs fluxes are evaluated from the Cs densities measured by TDLAS at the end of the plasma exposure. For Cs fluxes lower than  $2 \times 10^{15} \text{ m}^{-2} \text{ s}^{-1}$  the work function increases up to 3.8 eV as shown in figure 2(b) after a plasma exposure of

4.5 h. At a continuous Cs flux of  $4.4 \times 10^{15} \text{ m}^{-2}\text{s}^{-1}$  (constant over the plasma operation), the incoming Cs flux is not yet enough to maintain the work function of bulk Cs, and a work function of 2.3 eV is achieved after 2 h and 20 min. Instead, a Cs flux of  $1.5 \times 10^{16} \text{ m}^{-2}\text{s}^{-1}$  is sufficient to maintain a work function of 2.1 eV during long plasma operation.

### 3.4. Considerations for ion sources

The measurements at ACCesS show that for a fresh Cs layer a work function of 2.1 eV is achieved already in the first seconds of plasma exposure, and this can thus explain why at negative ion sources good performance is achieved for short pulses or at the beginning of long pulses [12]. Nonetheless, the work function can change during long plasma exposure and the results presented here indicate that there is a Cs flux threshold above which the work function can be maintained equal to 2.1 eV. In order to transfer the results to the ion sources, few considerations must be first done. At ELISE, up to 70% of the total Cs density close to the plasma grid is ionized [37], however the flux of  $\text{Cs}^+$  onto the plasma grid is strongly affected by the potential difference between the plasma and the plasma grid, which is usually positively biased with respect to the source walls. The  $\text{Cs}^+$  flux becomes negligible already for potential differences of few volts [37], and the main contribution to the Cs flux onto the plasma grid would be thus given by neutral Cs. The neutral Cs flux is typically around  $5\text{--}10 \times 10^{16} \text{ m}^{-2}\text{s}^{-1}$  at the beginning of the plasma pulse, and then it decreases to values around few  $10^{16} \text{ m}^{-2}\text{s}^{-1}$  [13, 37]. Such Cs flux would be enough at ACCesS, however it seems to be not the case at the ion source since the co-extracted electron current strongly increases during the long plasma pulse, suggesting a variation of the work function. This would mean that the threshold at the ion source is higher with respect to ACCesS. Unfortunately, the actual processes responsible of the Cs removal (which then determines the threshold) are not yet identified. Nonetheless, from the current investigations thermal desorption and physical sputtering do not seem to be the driving processes, while chemical processes and photo-induced reactions can have a role. The fluxes of hydrogen atoms and positive ions are higher at the ion sources with respect to ACCesS (up to a factor of 5 for  $\Gamma_{\text{H}}$  and up to one order of magnitude for  $\Gamma_{+}$ ), and very recent measurements reveal that the VUV photon flux is around one order of magnitude higher at the ion source [38]. The higher fluxes would thus lead to an enhanced Cs removal and, as a consequence, would explain why a higher Cs flux is necessary to counteract the removal at the ion source.

Additionally, the ion source performance during long pulse operation decreases much faster in deuterium [12]. From investigations performed with hydrogen and deuterium plasmas at 0.6 Pa [5, 39], it can be estimated that at 0.6 Pa similar atomic fluxes are achieved with the two isotopes in the driver region (where the plasma is generated), since the higher density observed in deuterium is compensated by a lower thermal velocity. The positive ion density is more homogeneous over the plasma grid area, increasing the average positive ion flux of almost a factor of two in deuterium with respect to hydrogen. The same behavior of the fluxes when switching from hydrogen to deuterium can be expected also at 0.3 Pa. In fact, first measurements show that the atomic flux in hydrogen is similar to the one in deuterium also at this pressure [40]. Further investigations at 0.3 Pa are ongoing, and a higher flux of positive ions (or of the photons) might explain the faster degradation of the performance in deuterium.

Finally, the results presented in the current contribution indicate that higher Cs fluxes are needed in order to maintain the Cs coverage on the plasma grid, assuring a homogeneous and temporally stable work function during long pulse operation. However, there is a limitation for the Cs flux due to Cs leaking through the grids of the extraction system, causing high voltage breakdowns between the grids [12]. A compromise is needed, and the open question is how to get enough Cs flux on the plasma grid without damaging the extraction system.

## 4. Summary and conclusion

A hydrogen and deuterium plasmas at 10 Pa and 250 W are applied at ACCesS to irradiate a freshly caesiated stainless steel sample, monitoring its work function. A work function of 2.1 eV is already achieved in the first 5–10 s of plasma, but then the work function changes for longer plasma exposure if no fresh Cs is further evaporated. The work function first decreases, and a minimum value of 1.8–1.9 eV is measured after 10–15 min of plasma. Then the work function increases up to values close to the work function of clean stainless steel ( $\geq 4.2$  eV) after 5 h. Hence, the Cs deposited on the sample is gradually removed by the plasma, and the low work function is lost. To counteract the Cs removal and to maintain a temporally stable surface work function of 2.1 eV during long plasma exposure, a minimum flux of fresh Cs towards the surface must be ensured, and a threshold of  $1.5 \times 10^{16} \text{ m}^{-2}\text{s}^{-1}$  is found. For ion sources this would mean that the work function of bulk Cs can be achieved for short pulses and at the beginning of long plasma pulses, but then it might be lost because the Cs flux onto the plasma grid is not sufficient to maintain the low work function of 2.1 eV.

## Acknowledgments

This work has been carried out within the framework of the EUROfusion Consortium and has received funding from the Euratom research and training programme 2014–2018 and 2019–2020 under grant agreement No 633053. The views and opinions expressed herein do not necessarily reflect those of the European Commission.

## ORCID iDs

S Cristofaro  <https://orcid.org/0000-0001-5395-9598>

R Friedl  <https://orcid.org/0000-0002-5723-994X>

U Fantz  <https://orcid.org/0000-0003-2239-3477>

## References

- [1] IAEA 2002 *ITER Technical Basis (ITER EDA documentation series 24)* (Vienna: International Atomic Energy Agency)
- [2] Hemsworth R et al 2009 *Nucl. Fusion* **49** 045006
- [3] Hemsworth R S et al 2017 *New J. Phys.* **19** 025005
- [4] Bacal M and Wada M 2015 *Appl. Phys. Rev.* **2** 021305
- [5] Heinemann B, Fantz U, Kraus W, Schiesko L, Wimmer C, Wunderlich D, Bonomo F, Fröschle M, Nocentini R and Riedl R 2017 *New J. Phys.* **19** 015001
- [6] Tsumori K et al 2012 *Rev. Sci. Instrum.* **83** 02B116
- [7] Michaelson H B 1977 *J. Appl. Phys.* **48** 4729
- [8] Wilson R G 1966 *J. Appl. Phys.* **37** 3161
- [9] Wilson R G 1966 *J. Appl. Phys.* **37** 4125
- [10] Swanson L W and Strayer R W 1968 *J. Chem. Phys.* **48** 2421
- [11] Fantz U et al 2017 *Nucl. Fusion* **57** 116007
- [12] Kraus W, Wunderlich D, Fantz U, Heinemann B, Bonomo F and Riedl R 2018 *Rev. Sci. Instrum.* **89** 052102
- [13] Wimmer C, Mimo A, Lindauer M, Fantz U, the NNBI Team and 2018 *AIP Conf. Proc.* **2011** 060001
- [14] Briefi S, Fantz U, the NNBI Team and 2018 *AIP Conf. Proc.* **2052** 040005
- [15] Fantz U and Briefi S 2018 Spectroscopic Investigations of the Ion Source at BATMAN Upgrade VI *International Symposium NIBS'18 (Novosibirsk, Russia)* - unpublished (talk)
- [16] Schiesko L, Wimmer C and Fantz U 2018 *AIP Conf. Proc.* **2052** 040006
- [17] McNeely P, Dudin S V, Christ-Koch S, Fantz U, the NNBI Team and 2009 *Plasma Sources Sci. Technol.* **18** 014011
- [18] Fantz U, Briefi S, Rauner D and Wunderlich D 2016 *Plasma Sources Sci. Technol.* **25** 045006
- [19] Gutser R, Fantz U and Wunderlich D 2010 *Rev. Sci. Instrum.* **81** 02A706
- [20] Mori Y, Okuyama T, Takagi A and Yuan D 1991 *Nucl. Instrum. Methods Phys. Res. A* **301** 1
- [21] Shinto K, Okumura Y, Ando T, Wada M, Tsuda H, Inoue T, Miyamoto K and Nagase A 1996 *Jpn. J. Appl. Phys.* **35** 1894
- [22] Hanada M, Seki T, Takado N, Inoue T, Mizuno T, Hatayama A, Kashiwagi M, Sakamoto K, Taniguchi M and Watanabe K 2006 *Nucl. Fusion* **46** S318
- [23] Morishita T, Kashiwagi M, Hanada M, Okumura Y, Watanabe K, Hatayama A and Ogasawara M 2001 *Jpn. J. Appl. Phys.* **40** 4709
- [24] Friedl R and Fantz U 2017 *J. Appl. Phys.* **122** 083304
- [25] Cristofaro S, Friedl R and Fantz U 2017 *AIP Conf. Proc.* **1869** 030036
- [26] Fantz U, Friedl R and Fröschle M 2012 *Rev. Sci. Instrum.* **83** 123305
- [27] Fantz U and Wimmer C 2011 *J. Phys. D: Appl. Phys.* **44** 335202
- [28] Cristofaro S 2019 Work function of caesiated surfaces in H<sub>2</sub>/D<sub>2</sub> low temperature plasmas correlated with negative ion formation *PhD Thesis* University of Augsburg
- [29] Fantz U, Falter H, Franzen P, Wunderlich D, Berger M, Lorenz A, Kraus W, McNeely P, Riedl R and Speth E 2006 *Nucl. Fusion* **46** S297
- [30] Friedl R and Fantz U 2013 *AIP Conf. Proc.* **1515** 255
- [31] Fowler R H 1931 *Phys. Rev.* **38** 45
- [32] Friedl R 2016 *Rev. Sci. Instrum.* **87** 043901
- [33] Songster J and Pelton A D 1994 *J. Phase Equilibria* **15** 84
- [34] Chase M W 1998 *NIST-JANAF Thermochemical Tables (IV ed J. Phys. Chem. Ref. Data, Monograph 9)* (Gaithersburg, MD: National Institute of Standards and Technology)
- [35] Ernst-Vidalis M L, Kamaratos M and Papageorgopoulos C 1987 *Surf. Sci.* **189–190** 276
- [36] Kudriavtsev Y, Villegas A, Godines A and Asomoza R 2005 *Appl. Surf. Sci.* **239** 273
- [37] Mimo A, Wimmer C, Wunderlich D and Fantz U 2018 *AIP Conf. Proc.* **2052** 040009
- [38] Fröhler-Bachus C 2020 *Private Communication* University of Augsburg
- [39] Fantz U, Schiesko L, Wunderlich D, the NNBI Team and 2013 *AIP Conf. Proc.* **1515** 187
- [40] Giacomini M 2017 Application of collisional radiative models for atomic and molecular hydrogen to a negative ion source for fusion *Master's Thesis* University of Padova